01 Sep 2010

Sensitivity of Geoelectrical Measurements to the Presence of Bacteria in Porous Media

Gamal Z. Abdel Aal

Estella A. Atekwana
Missouri University of Science and Technology, atekwana@mst.edu

Silvia Rossbach

D. Dale Werkema

Recommended Citation

G. Z. Abdel Aal et al., "Sensitivity of Geoelectrical Measurements to the Presence of Bacteria in Porous Media," *Journal of Geophysical Research*, vol. 115, no. 3, American Geophysical Union (AGU), Sep 2010. The definitive version is available at https://doi.org/10.1029/2009JG001279

Sensitivity of geoelectrical measurements to the presence of bacteria in porous media

Gamal Z. Abdel Aal,[1,2] Estella A. Atekwana,[1] Silvia Rossbach,[3] and Dale D. Werkema[4]

Received 30 December 2009; revised 17 March 2010; accepted 16 April 2010; published 19 August 2010.

[1] We investigated the sensitivity of low-frequency electrical measurements (0.1–1000 Hz) to (1) microbial cell density, (2) live and dead cells, and (3) microbial attachment onto mineral surfaces of clean quartz sands and iron oxide–coated sands. Three strains of *Pseudomonas aeruginosa* PAO1 (wild type and *rhlA* and *pilA* mutant) with different motility and attachment properties were used. Varying concentrations of both live and dead cells of *P. aeruginosa* wild type in sand columns showed no effect on the real conductivity component (σ'). However, the imaginary conductivity component (σ'') increased linearly with increasing concentrations of live cells in sand columns, whereas minimal changes were observed with different concentrations of dead cells. A strong power law relationship was observed between σ'' and the number of cells adsorbed onto sand grain surfaces with the *rhlA* mutant of *P. aeruginosa* displaying a higher power law exponent compared to the wild type and *pilA* mutant. In addition, power law exponents were greater in columns with iron oxide–coated sands compared to clean quartz sands. Minimal changes were observed on the σ' due to the attachment of *P. aeruginosa* cells onto sands. We relate the measured low-frequency electrical responses to (1) the distinct electrical properties of live cells and (2) the density of cells attached to mineral surfaces enhancing the surface roughness of sand grains and hence the polarization response. The information obtained from this study enhances our interpretation of microbially induced geoelectrical responses in biostimulated geologic media and may have implications for microbial transport studies.

Citation: Abdel Aal, G. Z., E. A. Atekwana, S. Rossbach, and D. D. Werkema (2010), Sensitivity of geoelectrical measurements to the presence of bacteria in porous media, *J. Geophys. Res.*, *115*, G03017, doi:10.1029/2009JG001279.

1. Introduction

[2] Microorganisms are ubiquitous and exist in the subsurface environment as plankton cells or adhered to mineral surfaces of porous media with abundance varying according to the availability of organic matter, water, and nutrients [*Hazen et al.*, 1991; *Balkwill and Boone*, 1997; *Konhauser*, 2007]. The microbial cells have distinct electrical properties that probably influence geoelectrical measurements (e.g., the effect of attachment-detachment of bacteria on mobility and zeta potential). It is known that microbial surfaces can develop a significant net surface charge as a result of protonation/deprotonation of carboxylates, phosphates, or other functional groups in their cell envelope [*Wasserman and Felmy*, 2000]. The net surface charge of bacterial cells results in the formation of an electric double layer, which is subjected to polarization when an electric current is applied. It has been recognized that the ion selectivity of the membranes of live bacterial cells in solution can generate a large polarization at low frequencies (<1000 Hz) [*Prodan et al.*, 2004, 2008].

[3] Bacterial adhesion/attachment to material surfaces is a complicated process that is influenced by several factors, including some characteristics of the bacteria themselves (e.g., hydrophobicity and surface charge), the environment (e.g., temperature, pH, ionic strength, bacterial concentrations, and exposure time), and the target materials (e.g., surface chemical composition, surface roughness, surface configuration, and surface hydrophobicity or wettability) [*An and Friedman*, 1998; *Kang and Choi*, 2005; *Roosjen et al.*, 2006; *Jiang et al.*, 2007]. Charge transfer between bacteria and conducting or semiconducting surfaces is known to play a very important role for the initial microbial adhesion [*Poortinga et al.*, 2002]. The charge transfer at the bacteria-substrate interface depends on the surface potential and ionic strength of the suspending medium and has been measured using electrochemical impedance spectroscopy [*Poortinga et al.*, 2002; *Bayoudh et al.*, 2008]. Therefore, it is believed that the distinct electrical properties of bacterial cells and

[1] Boone Pickens School of Geology, Oklahoma State University, Stillwater, Oklahoma, USA.
[2] Geology Department, Faculty of Science, Assiut University, Assiut, Egypt.
[3] Department of Biological Sciences, Western Michigan University, Kalamazoo, Michigan, USA.
[4] U.S. Environmental Protection Agency, Las Vegas, Nevada, USA.

0148-0227/10/2009JG001279

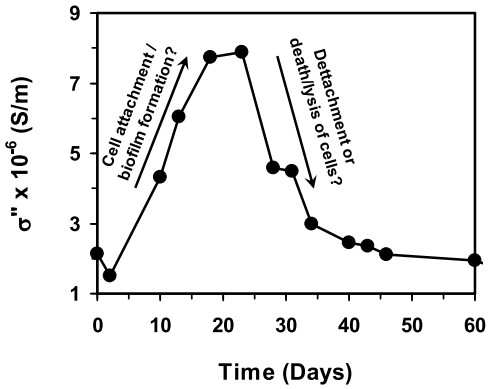

Figure 1. Temporal change in polarization response represented by imaginary conductivity component (σ'') at 2 Hz of biostimulated column as observed and hypothetically interpreted by *Davis et al.* [2006].

the charge transfer process during their initial attachment to mineral surfaces have the potential to impact the bulk electrical properties of the subsurface environment.

[4] There is a growing interest in the field of biogeophysics that combines the fields of environmental microbiology, biogeosciences, and geophysics to understand the electrical properties of microbial cells in porous media (see *Atekwana and Slater* [2009] for a review). Several laboratory experiments have been conducted to investigate the direct geophysical response of microbial cell concentration [*Ntarlagiannis et al.*, 2005] and the growth of cells and their attachment to porous media surfaces [*Davis et al.*, 2006, 2009; *Abdel Aal et al.*, 2006, 2009]. All of these investigations showed an enhancement of polarization due to alteration of mineral-fluid interface at low microbial cell densities [*Ntarlagiannis et al.*, 2005], pore clogging due to higher microbial cell densities [*Ntarlagiannis et al.*, 2005], biofilm formation [e.g., *Davis et al.*, 2006; *Abdel Aal et al.*, 2006], or cell attachment to mineral surfaces [*Abdel Aal et al.*, 2009].

[5] In particular, *Davis et al.* [2006] found significant changes in the polarization response of a biostimulated column coinciding in time with changes in concentration of cells attached to the sand surface. The results showed that the peak in polarization (at 2 Hz frequency) represented by the imaginary conductivity component (σ'') was coincident with the peak in microbial density and biofilm formation to mineral surfaces (Figure 1). The authors attributed the increase in polarization response within the first 20 days of their experiment to growth, attachment, and formation of biofilms and attributed the later decrease in polarization response toward the end of their experiment to detachment and death of cells. However, it was unclear from the *Davis et al.* [2006] study whether the source of the polarization is the electrical properties of the biofilm itself (i.e., direct detection) or the modification of the polarization associated with the porous medium as a result of cell attachment to mineral surfaces (i.e., indirect detection). *Abdel Aal et al.* [2009] further investigated the polarization response due to microbial attachment of *Pseudomonas aeruginosa* POA1 wild type onto clean quartz sands and iron oxide–coated sands. The authors observed that microbial adsorption to clean quartz sands was gradual and resulted in an increase of 13% in the imaginary conductivity component (σ''). However, when iron oxide–coated sands (20%–100% by weight) were used, a more rapid increase in microbial adsorption was observed with σ'' reaching a maximum of 37% increase for the 80%–100% iron oxide–coated sands.

[6] Microbial cells in the subsurface grow and die and attach to and detach from mineral surfaces according to changes in the subsurface environmental conditions such as temperature, osmolarity, pH, and nutrient availability [*Watnick and Kolter*, 2000; *Mai-Prochnow et al.*, 2004]. In addition, previous studies have also documented that under identical hydrodynamic and porous media conditions, microorganisms exhibit different attachment magnitudes even for the same organisms in different physiological states [*Grasso et al.*, 1996; *DeFlaun et al.*, 1999; *Chen and Strevett*, 2001]. Moreover, the presence of metal oxyhydroxide coatings has also been shown to result in greater attachment magnitudes of bacteria to sediment surfaces owing to the charge reversal imparted by the oxyhydroxide coatings at circumneutral pH [*Jiang et al.*, 2007]. Therefore, it is necessary to investigate the sensitivity of geophysical measurements to the presence of live or dead cells as well as the attachment of microbial cells with different properties (i.e., different attachment behavior) to mineral surfaces (with and without iron oxide coating) in porous media in order to enhance the interpretation of geophysical response data.

[7] In this study, we expand on the work of *Ntarlagiannis et al.* [2005], *Davis et al.* [2006], and *Abdel Aal et al.* [2009] by investigating the sensitivity of geophysical measurements to (1) different concentrations of microbial cells, (2) live and dead microbial cells, and (3) variations in the rate of microbial attachment onto clean quartz sands and iron oxide–coated sands based on differences in microbial genotypes. The results from this study demonstrate the extreme sensitivity of the low-frequency electrical measurements to the presence of microbial cells in porous media at different physiological states or genotypes (live versus dead cells or wild type versus mutant strains) with significant implications for the use of these techniques in microbial transport modeling studies.

2. Materials and Methods

[8] Two separate laboratory experiments were conducted to investigate the sensitivity of low-frequency electrical measurements to (1) different cell densities (live versus dead) and (2) variations in the magnitude of attachment of *P. aeruginosa* in saturated, sand-packed columns. The following is a brief description of the materials and experimental procedures for each experiment.

2.1. Column Construction and Setup

[9] Twenty-six identical columns were constructed and used for the cell density and microbial attachment experiments (Figure 2). Each of the experimental columns was constructed from polyvinyl chloride (PVC) pipe with an inner diameter of 3.17 cm and a length of 12 cm. Two nonpolarizing Ag-AgCl electrodes housed in electrolyte-filled chambers were placed 6 cm apart along the length of the column and not within the current flow path to avoid spurious polarization effect. Two Ag-AgCl coiled electrodes

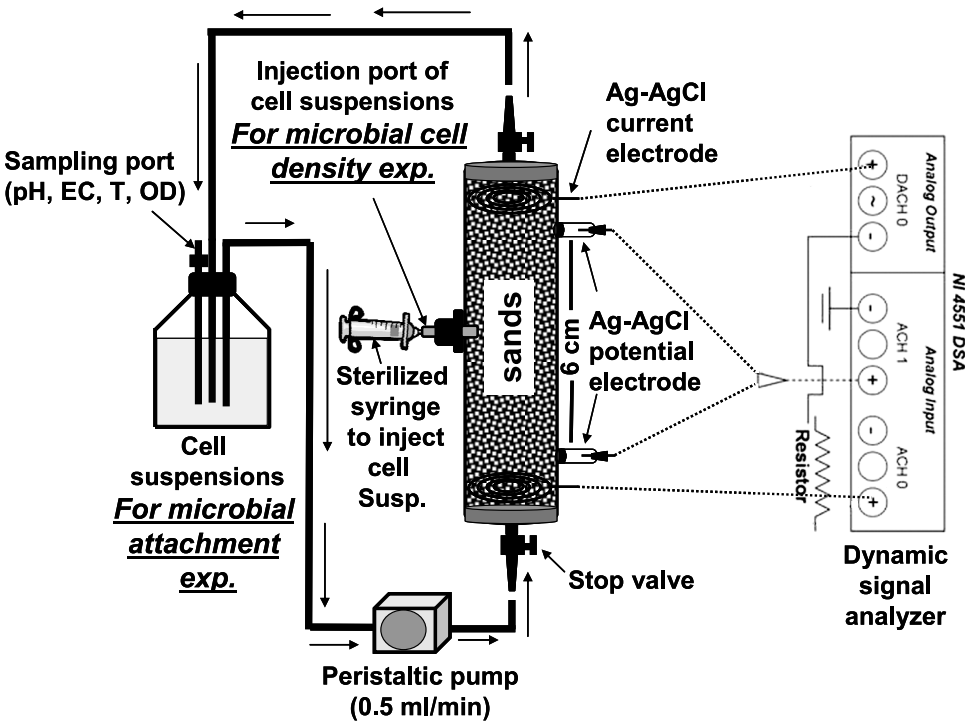

Figure 2. Schematic diagram showing the setup of the experimental columns used for microbial cell density experiment (live versus dead cells) and microbial attachment experiment. For the microbial cell density experiment, a syringe was used to inject the microbial cell suspensions into the sand columns through a Luer lock valve. For the microbial attachment experiment, a peristaltic pump was used to circulate the cell suspensions through the sand columns at a flow rate of 0.5 mL/min. A dynamic signal analyzer (DSA) was used to collect the low-frequency electrical measurements. EC, electrical fluid conductivity; T, temperature; OD, optical density.

were placed at either end of the column for one dimensional current injection. A two-channel dynamic signal analyzer (DSA) based around a National Instruments (NI) 4551 was used to perform the low-frequency electrical measurements between 0.1 and 1000 Hz at 40 equal logarithmic intervals [*Slater and Lesmes*, 2002]. The impedance magnitude $|\sigma|$ and the phase shift φ (between a measured voltage sinusoid and an impressed current sinusoid) of the sample were measured relative to a high-quality resistor. The real ($\sigma' = |\sigma| \cos \varphi$) and imaginary ($\sigma'' = |\sigma| \sin \varphi$) parts of the sample complex conductivity were then calculated. The real conductivity is an energy loss term that contains an electrolytic component (σ_{el}) and an interfacial component (σ'_{surf}) [e.g., *Lesmes and Frye*, 2001]. The σ'_{surf} results from surface conduction via the formation of an electrical double layer (EDL) at the grain-fluid interface [*Revil and Glover*, 1998]. The σ'' is an energy storage or polarization term, which at low frequencies (<1000 Hz) results primarily from the polarization of ions in the EDL at the mineral-fluid interface [*Lesmes and Frye*, 2001].

[10] An injection port was placed at the center of the columns and was used to inject the microbial cells for the cell density experiment. A sterilized syringe was used for this purpose. For the microbial attachment experiment, a peristaltic pump was used to deliver the cell suspensions (100 mL) from a sterilized flask to the sand columns and back to the flask again in a closed loop. All columns, tubing, and accessories were disinfected by rinsing in ethanol prior to the experiment.

2.2. Sand Preparation

[11] The sand used to fill the columns was purchased from U.S. Silica Company and was composed of 99.80% silicon dioxide, 0.02% iron oxide, 0.06% aluminum oxide, 0.01% titanium oxide, <0.01% calcium oxide, <0.01% magnesium oxide, <0.01% sodium oxide, and <0.01% potassium oxide. The particle diameters of the sands ranged between 500 and 710 μm. The sands were pretreated with hydrogen peroxide (6%) to remove organic matter; sodium acetate (pH 5) to remove carbonates; and a mixture of sodium citrate, sodium bicarbonate, and sodium hydrosulfite solution to remove iron oxides before being rinsed several times with deionized water (DIW), dried at 105°C, and autoclaved three times at 121°C for 30 min. A fraction of the pretreated sands was coated with iron oxide following the procedure of *Joshi and Chaudhuri* [1996] with some modifications as described previously by *Abdel Aal et al.* [2009]. In this procedure the pretreated sands were mixed with 2 M Fe $(NO_3)_3$ x $9H_2O$ solution adjusted to pH 11 using 10 M NaOH and then placed in a drying oven for 20 h. The dried iron oxide–coated sands were washed several times with DIW until the runoff was clear followed by oven drying at 110°C.

2.3. Bacterial Strains and Growth Conditions

[12] The strains of *P. aeruginosa* PAO1 used in our study were obtained from the University of Denmark, Lyngby, Denmark, where previous studies have been conducted [*Pamp and Tolker-Nielsen*, 2007]. *P. aeruginosa* is a gram-negative, 1 μm × 3 μm rod-shaped bacterium, with an estimated surface area of 25–30 μm^2. The strains were *P. aeruginosa* wild type (PAO1) and the PAO1-derived *rhlA* and *pilA* mutants. *P. aeruginosa* PAO1 was chosen because it is a ubiquitous bacterium: it occurs in soil and water, is associated with plants, and is an opportunistic human pathogen. Its ability to form biofilms is well researched, and mutant strains that differ in their ability to attach to surfaces are available [*Pamp and Tolker-Nielsen*, 2007]. Previous studies have indicated that the *P. aeruginosa* wild type is more efficient in forming a structured biofilm as compared to the *rhlA* and *pilA* mutants [*Pamp and Tolker-Nielsen*, 2007]. By analyzing the biofilm structure formed after 4 days, *Pamp and Tolker-Nielsen* [2007] observed that the wild type of *P. aeruginosa* PAO1 formed structured, mushroom-shaped biofilms. However, the *pilA* mutant strain formed irregular protruding structures, and the *rhlA* mutant strain formed flat biofilms. In another biofilm study by *Davey et al.* [2003], the results showed that the *rhlA* mutant strain was more effective in early colonization, with maximum attachment to microtiter dish at 24 h, which was twofold greater than the maximum observed for the wild type (maximum for the wild type was at 10 h).

[13] The *P. aeruginosa* strains were grown to stationary phase at 37°C in 30% Bushnell Hass (BH) broth (50 mg/L magnesium sulfate, 5 mg/L calcium chloride, 250 mg/L monopotassium phosphate, 250 mg/L diammonium hydrogen phosphate, 250 mg/L potassium nitrate, and 12.5 mg/L ferric chloride) (Becton, Dickinson and Company, Detroit, Michgan) and amended with 30 mmol glucose as a sole carbon source. The cells were centrifuged (4000 rpm, 50 min) and rinsed twice with filter-sterilized artificial ground water (AGW) similar to that used by *Abdel Aal et al.* [2009] to remove any remaining growth substrate (BH broth). The centrifuged cells were then prepared in different procedures to run the experiments as described in section 2.4. The *P. aeruginosa* wild-type strain was used in the microbial cell density experiment, and in addition to the *P. aeruginosa* wild type, the *rhlA* and *pilA* mutants were used in the microbial attachment experiment.

2.4. Experimental Procedures

[14] In this section we describe the experimental procedures for the two experiments conducted in this study.

2.4.1. Microbial Cell Density (Live Versus Dead)

[15] The centrifuged cells of the *P. aeruginosa* PAO1 were resuspended in 100 mL of filtered sterilized AGW with electrical fluid conductivity (EC) of 1000 ± 5.0 μS/cm, pH 7 ± 0.1, and a temperature (T) of 22°C ± 0.2°C in 250 mL flasks. Two sets of 10 flasks containing the cell suspensions were prepared with 10 different cell densities ranging from 0.31×10^9 to 5.0×10^9 colony-forming units (CFU)/ml. This range of microbial cell density was found to be relevant to the environmental abundance of *P. aeruginosa* PAO1 in natural sediments [*Roane and Pepper*, 2000]. The cell counts of each flask were determined by obtaining the optical density (OD) at 600 nm of the cell suspension with a spectrophotometer (AquaMate, Thermo Scientific). The OD_{600} (absorbance unit, AU) values were then converted into CFU/ml using the equation $CFU/mL = 5.40 \times 10^9 \times OD_{600}\ (AU) + 1.46 \times 10^8$; $R^2 = 0.98$, where R^2 is the regression coefficient. This equation was previously obtained and described by *Abdel Aal et al.* [2009] for the same bacterial species used in this study. One set of the 10 flasks contained preserved suspensions of live cells, and the second set contained dead cells (obtained by autoclaving the cell suspensions at 135° C for 30 min). The EC, pH, T, and cell counts of the fluid cell suspensions were maintained for both sets of the flasks.

[16] Similarly, two sets of 10 experimental columns (Figure 2) were prepared, sterilized using ethylene oxide and dry packed with the pretreated clean sands in a way that minimized grain sorting through gentle tapping of the columns. The porosity of the sand packed in each PVC column was calculated by relating column dimensions with measured weights of wet and dried sands. For these calculations a sand density of 2.65 g/cm^3 and water density of 1 g/cm^3 were assumed, and the porosity was calculated by subtracting the volume of sands from the total volume of the column. The porosity of sands packed in columns varied slightly for each column and was determined to be 0.42 ± 0.01 with a resulting pore volume being 39.78 ± 4.74 mL. Prior to the start of the experiment, the two sets of sand-packed columns were calibrated to investigate the effect of packing on the low-frequency electrical measurements. The calibration process was carried out by flushing the sand columns with 100 pore volume of filter-sterilized AGW similar to that used for cell suspensions, and low-frequency (0.1–1000 Hz) electrical measurements were obtained several times during the flushing process. The calibration process was accomplished with the EC and pH of the inlet and outlet AGW being the same, and the measured low-frequency electrical parameters were repeatable with less than 2% difference among columns. The experiment was started with the first set of flasks containing the live cell suspensions. Using a sterilized syringe, one pore volume was extracted from each flask and injected into a sand column (previously saturated with filter-sterilized AGW) through a Luer lock valve, followed by taking the low-frequency electrical measurements. The same procedure was repeated on the second set of experimental columns with the dead cell suspensions.

2.4.2. Microbial Attachment

[17] This experiment was conducted in two stages: in 250 mL flasks and in sand columns using the three above-described strains of live *P. aeruginosa* (wild type and *pilA* and *rhlA* mutants). The flask experiment was conducted prior to the sand column experiment in order to examine the difference in attachment magnitude between the different *P. aeruginosa* (wild type and *pilA* and *rhlA* mutants) strains to clean quartz sands and 100% iron oxide–coated sands. The flask experiment was conducted by adding 180 g of clean quartz sands plus 100 mL of bacterial cell suspensions into a 250 mL glass flask. The experiment was conducted for 140 min under static conditions (without shaking the flasks). Fluid and sand samples were extracted every 10 min for the first hour and then every 20 min for the next 80 min. The fluid samples were analyzed for cell counts following the

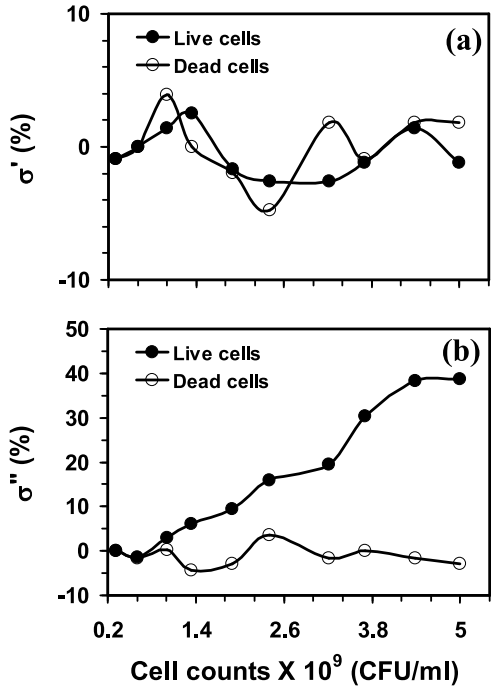

Figure 3. Percent change in (a) real conductivity (σ') and (b) imaginary conductivity (σ'') as a function of cell numbers of live or dead *P. aeruginosa* wild-type cells.

procedure outlined in the microbial cell density experiment in section 2.4.1. The number of the cells attached to mineral surfaces was determined by subtracting the number of cells at each sampling time from the number of cells in the initial suspension. The sand samples were fixed with 2.5% glutaraldehyde for later observation using an environmental scanning electron microscope. Images of the sand surfaces and attached microbial cells were obtained using an FEI Quanta 600 field emission gun integrated with electron backscattering diffraction system. The same procedure was repeated using 100% iron oxide–coated sands.

[18] The second phase of the microbial attachment experiment was conducted in prefabricated columns filled with sands (see section 2.1). A procedure similar to the flask experiment was followed. A peristaltic pump was used (Figure 2) to circulate the cell suspensions (100 mL with 1.9×10^9 CFU/mL of initial cell concentration) through the sand column at a flow rate of 0.5 ml/min. Fluid samples were extracted from the flask using the same time interval as for the flask experiment and were analyzed immediately for EC, pH, *T*, and cell counts. Cells attached to sand grain surfaces were determined in a similar manner as the flask experiment.

3. Results

3.1. Microbial Cell Density Experiment (Live Versus Dead)

[19] Figure 3 shows the percent changes in real (σ') and imaginary (σ'') conductivities as a function of cell counts (CFU/mL) of live or dead *P. aeruginosa* wild-type cells. We show the electrical data at 10 Hz, as this is the frequency at which our measurement error was lowest (less than 3% for phase measurements between 0.1 and 100 Hz). This error was previously obtained from low-frequency electrical measurements carried out on fluids with electrical conductivities matching those of the measured samples. No changes were observed in the shape of the σ' and σ'' spectra over time, and hence, we focus here on the percent change in the magnitude of the measured parameters. The σ' for both live and dead *P. aeruginosa* wild-type cells shows no consistent trend with increasing cell density with minimal percent changes (±4%) (Figure 3a). The σ'' component of live cells increased reaching a maximum percent change of 38% with increasing cell counts to 4.2×10^9CFU/mL (Figure 3b). Thereafter, σ'' remained steady with increasing cell counts to 5.0×10^9 CFU/mL. Increasing dead cell counts showed no significant changes in σ'' component (±4%) (Figure 3b).

[20] A correlation analysis of σ'' values at 10 Hz and live cell counts is shown in Figure 4. The data were fitted with a linear model using the least squares method. Figure 4 shows that σ'' varies linearly with live cell counts. The linear model is represented by the following equation: $\sigma'' \times 10^{-6}$ (S/m) = 0.16×10^9 (CFU/mL) + 1.66×10^8 with a strong regression coefficient ($R^2 = 0.97$).

3.2. Microbial Attachment Experiment

3.2.1. Flask Experiment

[21] Figures 5a and 5b show the temporal change in adsorption of *P. aeruginosa* wild-type and *pilA* and *rhlA* mutant cells onto clean quartz sands and 100% iron oxide–coated sands. For the clean quartz sands, the number of cells of the three strains of *P. aeruginosa* adsorbed onto sand surfaces increased gradually with time with the *rhlA* mutant showing the highest magnitude of attachment followed by the wild type and then the *pilA* mutant (Figure 5a). Similar observations were obtained using 100% iron oxide–coated sands but with a higher magnitude in the number of attached cells of the *rhlA* mutant as compared to clean quartz sands as shown in Figure 5b. However, the numbers of wild-type and *pilA* mutant strains attached to 100% iron oxide–coated sands were approximately similar to the number of cells attached to clean quartz sands.

[22] To verify the results presented in Figure 5, representative environmental scanning electron microscope (ESEM) images were collected from flasks containing the clean quartz sands. The representative ESEM images were

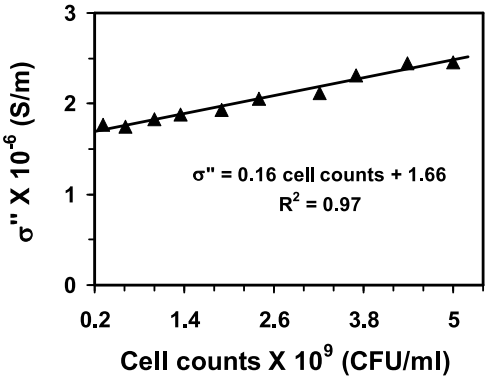

Figure 4. Cross correlation between imaginary conductivity (σ'') and cell numbers of live *P. aeruginosa* wild-type cells. The data were fitted with a linear model using the least squares method.

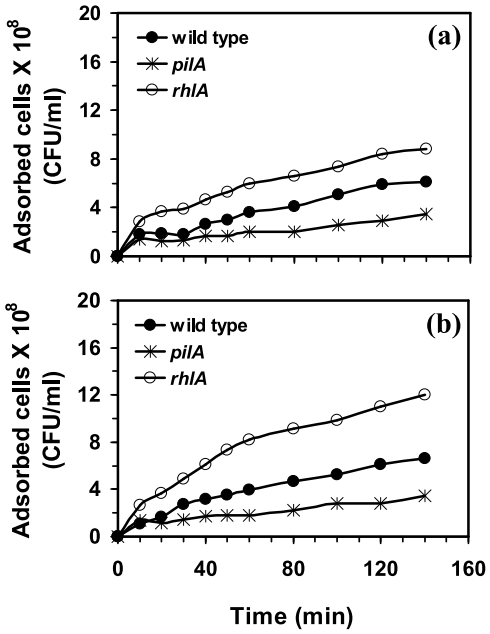

Figure 5. Temporal changes in adsorption of *P. aeruginosa* wild-type and *pilA* and *rhlA* mutant cells onto (a) clean quartz sands and (b) 100% iron oxide–coated sands. Results from flask experiment.

selected after spatial analysis (the spatial distribution and density of cells attached to different areas of sand grain surfaces) was conducted on random sand grain samples. Figure 6 displays representative ESEM images of sand grains collected at the end of the experiment showing a qualitative difference in the number of attached wild-type

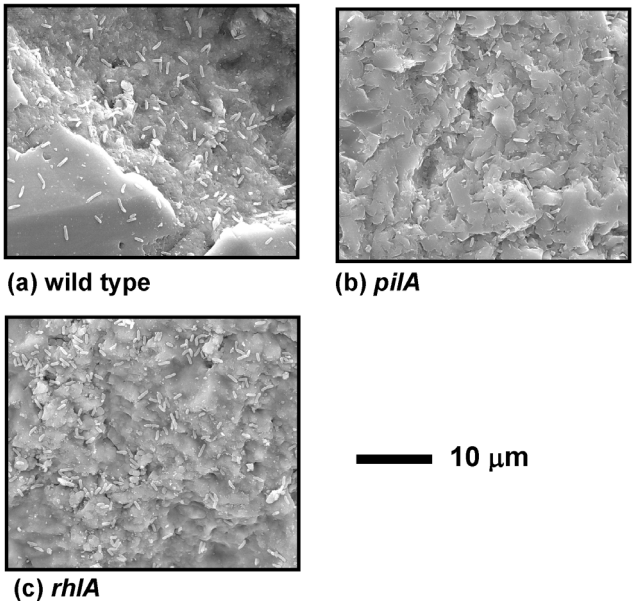

Figure 6. Selected environmental scanning electron microscope images of clean quartz sands at the end of the experiment. Notice the difference in densities of attached *P. aeruginosa* wild-type and *pilA* and *rhlA* mutant cells to sand grains.

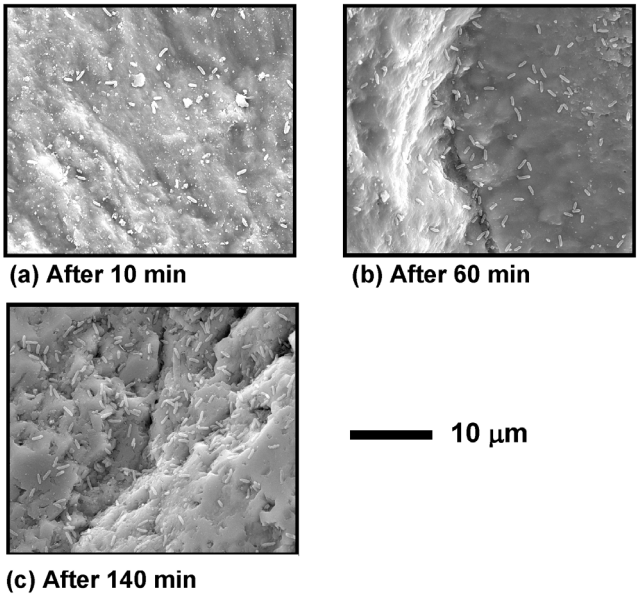

Figure 7. Selected environmental scanning electron microscope images of clean quartz sands with the *P. aeruginosa rhlA* mutant attached at different times of the experiment.

and *pilA* and *rhlA* mutant cells. It is clear that the number of cells of *rhlA* mutant attached to sand grain surfaces (Figure 6c) is greater than the wild type (Figure 6a) with the ESEM image of the *pilA* mutant showing the lowest number of attached cells (Figure 6b). Figure 7 displays representative ESEM images of sand grains obtained from the flasks containing the *rhlA* mutant cells to validate the observed increase in attached cells over time. The ESEM image after 10 min showed few cells attached to the surface of sand grains (Figure 7a). However, the number of attached cells increased with increasing time as displayed in Figure 7b (after 60 min) and Figure 7c (after 140 min).

3.2.2. Sand Column Experiment

[23] During the time span of the experiment, no significant changes were observed on the values of EC, pH, and *T* of the sampled fluids. Figures 8a and 8b show the temporal changes of *P. aeruginosa* wild-type and *pilA* and *rhlA* mutant cells adsorbed onto clean quartz sands and 100% iron oxide–coated sands, respectively. Again, the number of attached cells of all three strains increased with time, and the *rhlA* mutant cells displayed the highest magnitude of attachment compared to the wild type and the *pilA* mutant (Figures 8a and 8b). In addition, the magnitude of attachment of the three strains is relatively lower in columns filled with clean quartz sands (Figure 8a) than in columns filled with 100% iron oxide–coated sands (Figure 8b). The results are consistent, but the numbers are slightly greater than those obtained from the flask experiments.

[24] The results at 10 Hz of the low-frequency electrical measurements (σ' and σ'') are presented in Figures 9 and 10. Again, no changes were observed in the shape of the σ' and σ'' spectra over time, and hence, we focus here on the percent change in the magnitude of the measured parameters. Figure 9 shows minimal variation in percent changes in σ' (±4.8%) with time due to adsorption of the *P. aeruginosa*

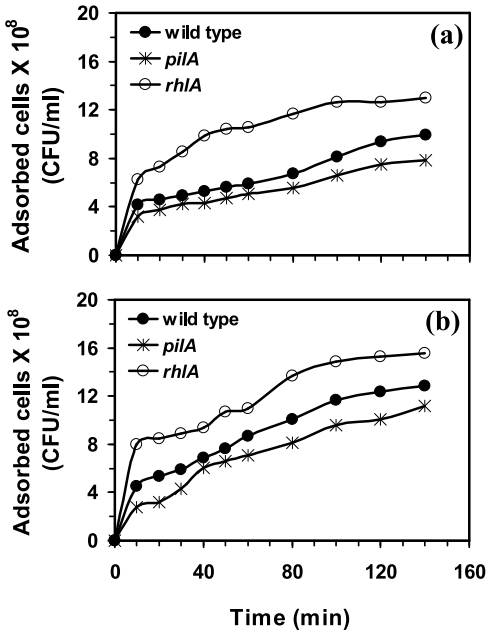

Figure 8. Temporal changes in adsorption of the *P. aeruginosa* wild-type and *pilA* and *rhlA* mutant cells onto (a) clean quartz sands and (b) 100% iron oxide–coated sands. Results from sand column experiment.

wild-type and *pilA* and *rhlA* mutant cells onto clean quartz (Figure 9a) and 100% iron oxide–coated sands (Figure 9b). The temporal percent change in σ'' due to adsorption of the *P. aeruginosa* wild-type and *pilA* and *rhlA* mutant cells onto

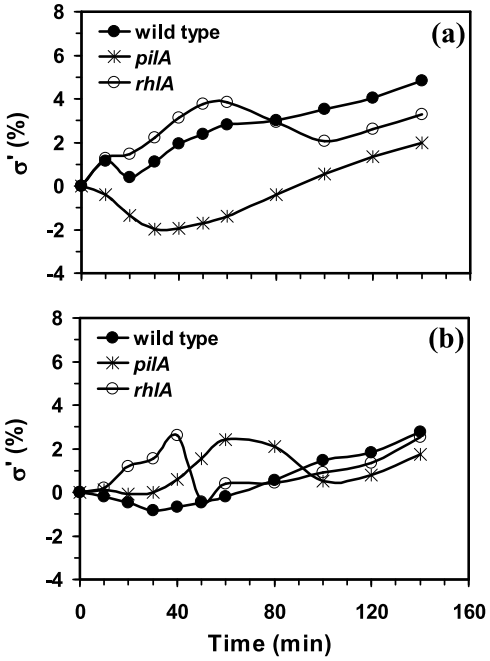

Figure 9. Temporal percent change in σ'' due to adsorption of the *P. aeruginosa* wild-type and *pilA* and *rhlA* mutant cells onto (a) clean quartz sands and (b) 100% iron oxide–coated sands.

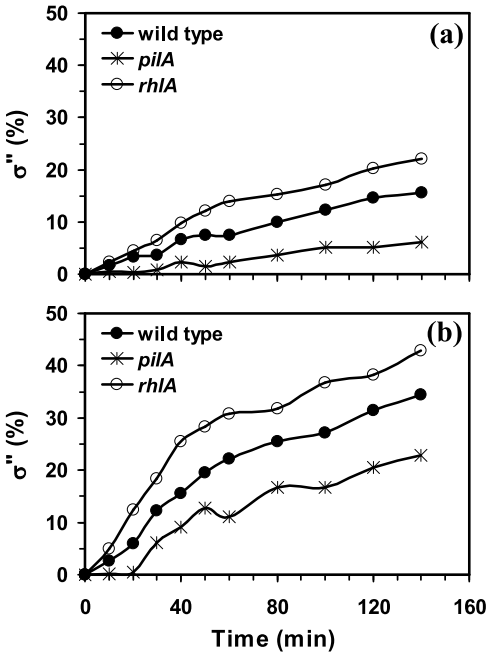

Figure 10. Temporal percent change in σ'' due to adsorption of the *P. aeruginosa* wild-type and *pilA* and *rhlA* mutant cells onto (a) clean quartz sands and (b) 100% iron oxide–coated sands.

clean quartz and 100% iron oxide–coated sands are shown in Figures 10a and 10b, respectively. In general, the σ'' increased with cell adsorption to sand grain surfaces as a function of time (Figures 10a and 10b). In addition, the magnitude of the σ'' response due to the adsorption of the *rhlA* mutant was relatively greater than that of the wild type, with the *pilA* mutant displaying the lowest σ'' magnitude (Figures 10a and 10b). The adsorption of *P. aeruginosa* cells onto clean quartz sands displayed a gradual increase in σ'' magnitude over time, reaching maximum percent changes of 22%, 16%, and 7% for the *rhlA* mutant, the wild type, and the *pilA* mutant, respectively. However, the adsorption of *P. aeruginosa* wild type and *pilA* and *rhlA* mutant cells onto 100% iron oxide–coated sands exhibited a rapid increase in the percent change of σ'' within the first 60 min of the experiment (Figure 10b). After 60 min, the adsorption of the *P. aeruginosa* cells onto 100% iron oxide–coated sands displayed a gradual increase in the percent change of σ'', reaching maximum values of 42%, 34%, and 23% for the *rhlA* mutant, the wild type, and the *pilA* mutant, respectively (Figure 10b).

[25] To further examine the sensitivity of the low-frequency electrical measurements to the magnitude of adsorbed microbial cells, a power law relationship was obtained between the values of adsorbed *P. aeruginosa* wild-type and *pilA* and *rhlA* mutant cells and the σ'' values at 10 Hz for both clean quartz and 100% iron oxide–coated sands. The power law exponents and regression coefficients obtained from the fitted models are summarized in Table 1. The *rhlA* mutant showed a higher power law exponent compared to the wild type and the *pilA* mutant as shown in Table 1. In addition, power law exponents were greater in columns with

Table 1. Regression Coefficients and Power Law Exponent Values Derived From the Regression Analysis of Imaginary Conductivity Versus Adsorbed Values of Microbial Cells[a]

Sand Type	Strain Type	Regression Coefficient R^2	Power Law Exponent
Clean quartz sands	wild type	0.98	0.15
	pilA	0.91	0.07
	rhlA	0.94	0.23
100% iron oxide–coated sands	wild type	0.98	0.24
	pilA	0.97	0.15
	rhlA	0.85	0.35

[a]Imaginary conductivity is measured in S/m, and adsorbed values are measured in CFU/mL.

100% iron oxide–coated sands compared to clean quartz sands (Table 1).

4. Discussion

4.1. Effects of Cell Density on Low-Frequency Electrical Properties

[26] Microbial cells have distinct electrical properties, and their attachment to mineral surfaces has the potential to impact electrical properties of the subsurface environment. Previous dielectric spectroscopy (analogous to electrical geophysical exploration methods) studies of cellular suspensions of living cells suggested that the finite membrane potential of the cells leads to a large dielectric response at low frequency (<10 Hz) in the presence of an electrical field [*Prodan et al.*, 2004; *Atekwana and Slater*, 2009]. We show in this study that low-frequency electrical measurements (e.g., σ'') in sand columns are sensitive to the concentrations of live *P. aeruginosa* cells and also to their magnitude of attachment on sand grain surfaces. Our results show that varying the concentrations of dead cell suspensions has minimal effect (±3%) on both the real (σ') and imaginary (σ'') conductivity components (Figures 3a and 3b). Increasing the concentrations of live cells had no significant impact on the σ' component; however, the imaginary conductivity component (σ''), being a direct measure of polarization, increased to a maximum of 40% from the initial values (1.77×10^{-6} S/m) (Figure 3b) and displayed a strong linear correlation to the number of cells attached (Figure 4). These results are consistent with previous results that showed a 15% increase in σ'' with increasing cell numbers of *Escherichia coli* being injected into columns filled with clean quartz sands [*Ntarlagiannis et al.*, 2005].

[27] In this study, the linear model obtained from the correlation between σ'' and the cell density of live *P. aeruginosa* cells can be used (under similar experimental conditions) to estimate the changes in σ'' due to the increase in microbial cells in the subsurface porous media. Surface conductivity is primarily controlled by the product of surface area, surface charge density, and surface ionic mobility [*Lesmes and Frye*, 2001; *Slater and Lesmes*, 2002; *Slater and Glaser*, 2003]. Bacteria have large surface areas and surface charge densities similar to clay particles [*Bickmore et al.*, 2002]. Therefore, the increase in microbial cell numbers in porous media may result in polarization enhancement due to the polarization of the electrical double layer of microbial cells when the electric field is applied. Therefore, the increase in σ'' with increasing concentration of live cells in suspensions is directly related to the electrical properties of microbial cells and to the enhancement in the interfacial electrical properties due to accumulation and interaction of charged microbial cells at the mineral-fluid interfaces.

[28] The electrical properties of microbial cell surfaces are related to the chemical compositions of the microbial cell walls with the membranes being permeable to ions in pore fluids [*Van Der Wal et al.*, 1997]. Therefore, breaking down the membranes of microbial cells will result in a loss of their electrical properties, which are manifested in the minimal σ'' response in our sand columns saturated with different concentrations of dead cell suspensions of *P. aeruginosa* wild type (Figure 3b). Previous studies have suggested that cell death, for example autolysis during biofilm development, is important to enhance the ability of other cells to disperse from within biofilms and colonize new surfaces [*Web et al.*, 2003; *Mai-Prochnow et al.*, 2006]. Therefore, we suggest that the results of the live-dead cell experiment can be used to explain the decrease in polarization response at the late stage of biofilm growth and development observed by *Davis et al.* [2006] (Figure 1).

4.2. Effect of Cell Attachment/Sorption to Mineral Surfaces on the Low-Frequency Electrical Properties

[29] Attachment of microbial cells onto mineral grain surfaces is controlled by several factors, including the mineralogy. For example, the presence of metal oxyhydroxide coatings on aquifer sediments can result in positively charged sediment surfaces, which increases the deposition rates of negatively charged bacterial cells [*Bolster et al.*, 2001; *Mills et al.*, 1994; *Yee et al.*, 2000; *Jiang et al.*, 2007]. We have shown previously in the *Abdel Aal et al.* [2009] study that increases in cell adsorption to mineral surfaces enhanced the polarization magnitude with the magnitude of the polarization being greater for iron oxide–coated sands compared to clean quartz sands. In this study, we wanted to investigate just how sensitive the low-frequency electrical methods are to the magnitude of cell deposition on mineral surfaces by investigating three different genotypes of *P. aeruginosa* (wild type and *pilA* and *rhlA* mutants) with different attachment abilities/magnitudes (Figure 5). Despite the fact that the wild type is more efficient in forming a structured biofilm compared to the *rhlA* and *pilA* mutants [*Pamp and Tolker-Nielsen*, 2007], both flask and sand column experiments showed that the *rhlA* mutant displayed a higher magnitude of attachment, followed by the wild type, with the *pilA* mutant showing the lowest attachment magnitude (Figures 5 and 8). These findings are supported by the representative ESEM images that show the relative difference in numbers of adsorbed wild-type and *pilA* and *rhlA* mutant cells onto mineral grain surfaces of clean quartz sands at the end of the experiment (Figure 6).

[30] Nevertheless, an *rhlA* mutant was found to be more proficient at early colonization of surfaces than the wild-type strain [*Davey et al.*, 2003]. Therefore, the difference in the magnitude of attachment between the three strains used in this study may be related to the difference in motility, which is considered to be one of the important factors affecting the

initial attachment of microbial cells onto mineral surfaces and development of biofilm structures [*Morisaki et al.*, 1999]. In addition, representative ESEM images of the *rhlA* mutant type document the temporal changes in adsorption magnitude at different times during the experiment (Figure 7). The temporal changes in adsorption of microbial cells over time are related to the increase in exposure time and collision events of microbial cells onto mineral grain surfaces [*Scheibe et al.*, 2007].

[31] The different attachment magnitudes of the three different *P. aeruginosa* strains onto mineral surfaces of clean quartz sands and 100% iron oxide–coated sands are also manifested in the magnitude of the σ'' component (Figures 10a and 10b). The *rhlA* mutant with a higher microbial attachment magnitude also displayed a higher σ'' magnitude compared to the wild type and the *pilA* mutant and was higher in columns with 100% iron oxide–coated sands compared to clean quartz sands (Figures 10a and 10b). These results demonstrate the dependency of the σ'' component on the number of microbial cells adsorbed to sand grain surfaces, which is consistent with previous findings by *Abdel Aal et al.* [2009]. These results were further supported by the strong power law relationship observed between σ'' and the number of cells adsorbed onto sand grain surfaces with the *rhlA* mutant of *P. aeruginosa* displaying a higher power law exponent compared to the wild type and the *pilA* mutant. In addition, power law exponents were greater in columns with 100% iron oxide–coated sands compared to clean quartz sands. The observed increase in σ'' due to the increase in the number of microbial cells adsorbed to sand grain surfaces can be explained by the increase in surface roughness of grains as suggested by *Abdel Aal et al.* [2009].

[32] On the basis of our results, it is apparent that microbial cell density, viable cells (live), and microbial attachment magnitude play an important role in the geoelectrical responses measured in biostimulated laboratory sand column experiments. We documented that an increase in viable microbial cell density and attachment onto mineral grain surfaces enhanced the interfacial electrical properties of porous media at the microbe-mineral-fluid interfaces. Nevertheless, the dead cells showed no effect on the interfacial electrical properties.

4.3. Implication for Microbial Transport and Biofilm Monitoring in Porous Media

[33] The transport, attachment, growth, and biofilm development of microorganisms in the subsurface is of great importance in a variety of applications and processes, such as for in situ bioremediation [e.g., *Steffan et al.*, 1999], microbially enhanced oil recovery [e.g., *Tanner et al.*, 1991], biostimulation [e.g., *MacDonald et al.*, 1999], bioaugmentation [e.g., *Witt et al.*, 1999], biobarrier technologies for containment of pollutants [e.g., *Stewart and Fogler*, 2002], and microbial facilitated transport of contaminants [e.g., *Kim et al.*, 2003]. These applications and processes require accurate prediction and monitoring of microorganisms in subsurface granular porous media. Conventional and traditional methods of documenting bacterial presence in natural environments and monitoring biofilm development usually involve the periodic sampling of representative sediments and time-consuming microbiological culturing techniques using destructive methods [*Cristiani et al.*, 2008]. Therefore, the development of alternative detection and identification technologies has become increasingly important in recent decades. Our results demonstrate the sensitivity of low-frequency electrical measurements to microbial cell densities and magnitude of attachment to mineral grain surfaces and hence have the potential to be used as a cost-effective and nondestructive method in microbial transport and biofilm monitoring processes and applications. For example, the sensitivity of the low-frequency electrical measurements to microbial cell densities encourages the application of the method in bioaugmentation processes as a complementary tool to make sure that effective concentrations of microorganisms are transported to contaminated areas of the subsurface to achieve desirable cleanup results. Similarly, the low-frequency electrical measurements can be used during microbially enhanced oil recovery, which requires monitoring of the growth of naturally occurring bacteria or injected bacteria to emulsify the heavy oil to be easily extracted.

[34] It is well documented that formation and development of biofilms occur in several stages from initial attachment to growth of microbial cells and colonization of mineral surfaces to a final maturation that may end up with increase in cell death or detachment of microbial cells according to environmental conditions [*Davey et al.*, 2003]. Our results demonstrate that low-frequency electrical measurements are sensitive to cell density and magnitude of attachment to mineral grains and hence can be used as a sensor to monitor different stages of biofilm development from changes in interfacial electrical properties at the microbe-mineral-fluid interfaces. Another important finding from the present study is the ability of low-frequency electrical measurements to differentiate between microbial genotypes according to their differences in motility and attachment magnitude to mineral grain surfaces. This information can be useful in studies related to modeling of microbial transport and attachment in biostimulated porous media.

5. Conclusions

[35] The results from this study demonstrate the sensitivity of low-frequency electrical measurements, specifically the imaginary conductivity component (σ'') to microbial cell density, live and dead cells, and magnitude of microbial attachment of *P. aeruginosa* PAO1 wild-type and *rhlA* and *pilA* mutant cells onto clean quartz sands and 100% iron oxide–coated sands. The σ'' component showed a strong dependency on the density of live microbial cells and the number of cells adsorbed to sand grain surfaces, with the magnitude being greater in columns filled with 100% iron oxide–coated sand. Dead microbial cells exhibit minimal changes in low-frequency electrical measurements in sand columns due to the loss of their electrical properties resulting from the breakdown of membranes. The enhancement in the low-frequency electrical properties (e.g., σ'') due to the increase in cell numbers and their attachment to mineral surfaces are related to (1) the distinct electrical properties of bacterial cells (e.g., electric double layer and charge transfer) and (2) increase in surface roughness of grains and hence the polarization response due to microbial attachment. We con-

clude that our low-frequency electrical measurements can be used to monitor microbial transport and biofilm development in subsurface porous media with some emphases on the application of the method in some environmental and engineering applications such as microbially enhanced oil recovery or in situ bioremediation processes.

[36] **Acknowledgments.** This material is based in part on work supported by the National Science Foundation under grant OCE-0729642 and DOE-BER grant DE-FG02-07ER64413. This work was partially funded through the U.S. Environmental Protection Agency through the student services contracts EP09D000547 and EP09D000553.Although this work was reviewed by the EPA and approved for presentation, it may not necessarily reflect official agency policy. Mention of trade names or commercial products does not constitute endorsement or recommendation by the EPA for use. The ESEM used for imaging was obtained through NSF-MRI grant EAR 0722410. We thank C. Ownby for help with ESEM imaging. We thank S. Pamp and T. Tolker-Nielsen for providing the *Pseudomonas* strain and Farag Mewafy, Matt Mcguire, and Dalton Hawkins for laboratory assistance.

References

Abdel Aal, G., L. D. Slater, and E. A. Atekwana (2006), Induced polarization measurements on unconsolidated sediments from a site of active hydrocarbon biodegradation, *Geophysics*, *71*, 13–24.

Abdel Aal, G., E. Atekwana, S. Radzikowski, and S. Rossbach (2009), Effect of bacterial adsorption on low frequency electrical properties of clean quartz sands and iron-oxide coated sands, *Geophys. Res. Lett.*, *36*, L04403, doi:10.1029/2008GL036196.

An, Y. H., and R. J. Friedman (1998), Concise review of mechanisms of bacterial adhesion to biomaterial surfaces, *J. Biomed. Mater. Res.*, *43*, 338–348.

Atekwana, E., and D. Slater (2009), Biogeophysics: A new frontier in earth science research, *Rev. Geophys.*, *47*, RG4004, doi:10.1029/2009RG000285.

Balkwill, D. L., and D. R. Boone (1997), Identity and diversity of microorganisms cultured from subsurface environments, in *The Microbiology of the Terrestrial Deep Surface*, edited by P. S. Amy and D. L. Haldeman, pp. 105–117, CRC Press, Boca Raton, Fla.

Bayoudh, S., A. Othmane, L. Ponsonnet, and H. B. Ouada (2008), Electrical detection and characterization of bacterial adhesion using electrochemical impedance spectroscopy-based flow chamber, *Colloids Surf. A*, *318*, 291–300.

Bickmore, B. R., K. L. Nagy, P. E. Sandlin, and T. S. Crater (2002), Quantifying surface areas of clays by atomic force microscopy, *Am. Mineral.*, *87*, 780–783.

Bolster, C. H., A. L. Mills, G. M. Hornberger, and J. S. Herman (2001), Effect of surface coatings, grain size, and ionic strength on the maximum attainable coverage of bacteria on sand surfaces, *J. Contam. Hydrol.*, *50*, 287–305.

Chen, G., and K. A. Strevett (2001), Impact of surface thermodynamics on bacterial transport, *Environ. Microbiol.*, *3*, 237–245.

Cristiani, P., A. Franzetti, and G. Bestetti (2008), Monitoring of electroactive biofilm in soil, *Electrochim. Acta*, *54*, 41–46.

Davey, M. E., N. C. Caiazza, and A. O. George (2003), Rhamnolipid surfactant production affects biofilm architecture in *Pseudomonas aeruginosa* PAO1, *J. Bacteriol.*, *185*, 1027–1036.

Davis, C. A., E. A. Atekwana, E. A. Atekwana, L. D. Slater, S. Rossbach, and M. R. Mormile (2006), Microbial growth and biofilm formation in geologic media is detected with complex conductivity measurements, *Geophys. Res. Lett.*, *33*, L18403, doi:10.1029/2006GL027312.

Davis, C. A., L. J. Pyrak-Nolte, E. A. Atekwana, D. D. Werkema, and M. E. Haugen (2009), Microbial-induced heterogeneity in the acoustic properties of porous media, *Geophys. Res. Lett.*, *36*, L21405, doi:10.1029/2009GL039569.

DeFlaun, M. F., S. R. Oppenheimer, S. Streger, C. W. Condee, and M. Fletcher (1999), Alterations in adhesion, transport, and membrane characteristics in an adhesion-deficient pseudomonad, *Appl. Environ. Microbiol.*, *65*, 759–765.

Grasso, D., B. F. Smets, K. A. Strevett, B. D. Machinist, C. J. VanOss, and R. F. Giese (1996), Impact of physiological state on surface thermodynamics and adhesion of *Pseudomonas aeruginosa*, *Environ. Sci. Technol.*, *30*, 3604–3608.

Hazen, T. C., L. Jimenez, and G. L. de Victoria (1991), Comparison of bacteria from deep subsurface sediment and adjacent ground water, *Microb. Ecol.*, *22*, 293–304.

Jiang, D., Q. Huang, P. Cai, X. Rong, and W. Chen (2007), Adsorption of *Pseudomonas putida* on clay minerals and iron oxide, *Colloids Surf. B*, *54*, 217–221.

Joshi, A., and M. Chaudhuri (1996), Removal of arsenic from groundwater using iron oxide-coated sands, *J. Environ. Eng.*, *122*, 769–771.

Kang, S., and H. Choi (2005), Effect of surface hydrophobicity on the adhesion of *S. cerevisiae* onto modified surfaces by poly(styrene-ransulfonic acid) random copolymers, *Colloids Surf. B*, *46*, 70–77.

Kim, S. B., M. Y. Corapcioglu, and D. J. Kim (2003), Effect of dissolved organic matter and bacteria on contaminant transport in riverbank filtration, *J. Contam. Hydrol.*, *66*, 1–23.

Konhauser, K. (2007), *Introduction to Geomicrobiology*, 425 pp, Blackwell Sci., Malden, Mass.

Lesmes, D. P., and K. M. Frye (2001), Influence of pore fluid chemistry on the complex conductivity and induced polarization responses of Berea sandstone, *J. Geophys. Res.*, *106*(B3), 4079–4090.

MacDonald, T. R., P. K. Kitanidis, P. L. McCarty, and P. V. Roberts (1999), Mass transfer limitations for macroscale bioremediation modeling and implications on aquifer clogging, *Ground Water*, *37*, 523–531.

Mai-Prochnow, A., F. Evans, D. Dalisay-Saludes, S. Stelzer, S. Egan, S. James, J. S. Webb, and S. Kjelleberg (2004), Biofilm development and cell death in the marine bacterium *Pseudoalteromonas tunicata*, *Appl. Environ. Microbiology*, *70*, 3232–3238.

Mai-Prochnow, A., J. S. Web, B. C. Ferrari, and S. Kjelleberg (2006), Ecological advantages of autolysis during the development and dispersal of *Pseudoalteromonas tunicata* biofilms, *Appl. Environ. Microbiol.*, *72*, 5414–5420.

Mills, A. L., J. S. Herman, G. M. Hornberger, and T. H. DeJesus (1994), Effect of solution ionic strength and iron coatings on mineral grains on the sorption of bacterial cells to quartz sand, *Appl. Environ. Microbiol.*, *60*, 3300–3306.

Morisaki, H., S. Nagai, H. Ohshima, E. Lkemoto, and K. Kogure (1999), The effect of motility and cell-surface polymers on bacterial attachment, *Microbiol.*, *145*, 2795–2802.

Ntarlagiannis, D., N. Yee, and L. Slater (2005), On the low frequency induced polarization of bacterial cells in sands, *Geophys. Res. Lett.*, *32*, L24402, doi:10.1029/2005GL024751.

Pamp, S. J., and T. Tolker-Nielsen (2007), Multiple roles of biosurfactants in structural biofilm development by *Pseudomonas aeruginosa*, *J. Bacteriol.*, *189*, 2531–2539, doi:10.1128/JB.01515-06.

Poortinga, A. T., R. Bos, W. Norde, and H. J. Busscher (2002), Electrical double layer interactions in bacterial adhesion to surfaces, *Surf. Sci. Rep.*, *47*, 3–32.

Prodan, C., F. Mayo, J. Claycomb, J. H. Miller, and M. J. Benedik (2004), Low-frequency, low-field dielectric spectroscopy of living cell suspensions, *J. Appl. Phys.*, *95*, 3754–3756.

Prodan, E., C. Prodan, and J. H. Miller (2008), The dielectric response of spherical live cells in suspension: An analytic solution, *Biophys. J.*, *95*, 4174–4182.

Revil, A., and P. W. J. Glover (1998), Nature of surface electrical conductivity in natural sands, sandstones, and clays, *J. Geophys. Res.*, *103*(B10), 23,925–23,936.

Roane, T. M., and I. L. Pepper (2000), Microbial response to environmentally toxic cadmium, *Microb. Ecol.*, *38*, 358–364.

Roosjen, A., H. J. Busscher, W. Norde, and H. C. van der Mei (2006), Bacterial factors influencing adhesion of *Pseudomonas aeruginosa* strains to a poly(ethylene oxide) brush, *Microbiology*, *152*, 2673–2682.

Scheibe, T. D., H. Dong, and Y. Xie (2007), Correlation between attachment rate coefficients and hydraulic conductivity and its effect on field-scale bacteria transport, *Adv. Water Resour.*, *30*, 1571–1582.

Slater, L., and D. Glaser (2003), Controls on induced-polarization in sandy unconsolidated sediments and application to aquifer characterization, *Geophysics*, *68*, 1547–1558.

Slater, L., and D. P. Lesmes (2002), IP interpretation in environmental investigations, *Geophysics*, *67*, 77–88.

Steffan, R. J., K. L. Sperry, M. T. Walsh, S. Vainberg, and C. W. Condee (1999), Field scale evaluation of in situ bioaugmentation for remediation of chlorinated solvents in groundwater, *Environ. Sci. Technol.*, *33*, 2771–2781.

Stewart, T. L., and H. S. Fogler (2002), Pore-scale investigation of biomass plug development and propagation in porous media, *Biotechnol. Bioeng.*, *77*, 577–588.

Tanner, R. S., E. O. Udegbunam, M. J. McInerney, and R. M. Knapp (1991), Microbially enhanced oil-recovery from carbonate reservoirs, *Geomicrobiol. J.*, *9*(4), 169–195.

Van Der Wal, A., M. Minor, W. Norde, A. J. B. Zehnder, and J. Lyklema (1997), Conductivity and dielectric dispersion of gram-positive bacterial cells, *J. Colloid Interface Sci.*, *186*, 71–79.

Wasserman, E., and A. R. Felmy (2000), Modeling the electrical double layer on microbial surfaces: Equilibrium and non-equilibrium treatments, paper presented at From Atoms to Organisms (and Back): Rates and Mechanisms of Geochemical Processes, Dep. of Energy, Gaithersburg, Md., 15–16 Oct.

Watnick, P., and R. Kolter (2000), Biofilm, city of microbes, *J. Bacteriol.*, *182*, 2675–2679.

Web, J. S., L. S. Thompson, S. James, T. Charlton, T. Tolker-Nielsen, B. Koch, M. Givskov, and S. Kjelleberg (2003), Cell death in *Pseudomonas aeruginosa* biofilm development, *J. Bacteriol.*, *185*, 4585–4592.

Witt, M. E., M. J. Dybas, D. C. Wiggert, and C. S. Criddle (1999), Use of bioaugmentation for continuous removal of carbon tetrachloride in model aquifer columns, *Environ. Eng. Sci.*, *16*(6), 475–485.

Yee, N., J. B. Fein, and C. J. Daughney (2000), Experimental study of the pH, ionic strength, and reversibility behavior of bacteria-mineral adsorption, *Geochim. Cosmochim. Acta*, *64*, 609–617.

G. Z. Abdel Aal and E. A. Atekwana, Boone Pickens School of Geology, Oklahoma State University, Stillwater, OK 74078, USA. (estella.atekwana@okstate.edu)

S. Rossbach, Department of Biological Sciences, Western Michigan University, Kalamazoo, MI 49008-5410, USA.

D. D. Werkema, U.S. Environmental Protection Agency, 944 E. Harmon Ave., Las Vegas, NV 89119, USA.